Histol Histopathol (2023) 38: 559-570

http://www.hh.um.es

Histology and Histopathology
From Cell Biology to Tissue Engineering

ORIGINAL ARTICLE **Open Access**

Hsa_circ_0093741 competes with FRS2 for miR-562 binding sites to promote nephroblastoma progression

Jiang Yong, Jun He and Feng Ning

Department of Urology, Hunan Children's Hospital, the Paediatric Academy of University of South China Changsha, Hunan, PR China

Summary. Background. Circular RNA (circRNA) has been shown to play an essential role in cancer progression, including nephroblastoma. Hsa_circ_0093741 was discovered to be highly expressed in nephroblastoma. However, its function and mechanism in nephroblastoma development are still vague.

Methods. The expression levels of hsa_circ_0093741, miR-562 and FRS2 (Fibroblast Growth Factor Receptor Substrate 2) were detected using western blotting and quantitative real-time polymerase chain reaction. Functional experiments were performed by using cell counting kit-8, colony formation, 5-ethynyl-2'-deoxyuridine (EdU), transwell, scratch assays in vitro and animal experiments *in vivo*. The interaction analysis was conducted using dual-luciferase reporter assay and RIP assay.

Results. Hsa_circ_0093741 was highly expressed in nephroblastoma tissues and cells. Functionally, hsa_circ_0093741 silencing significantly suppressed the growth, invasion, and migration of nephroblastoma cells *in vitro*. MiR-562 was decreased in nephroblastoma, and was validated to be a target of hsa_circ_0093741. Inhibition of miR-562 reversed the anticancer functions of hsa_circ_0093741 silencing on nephroblastoma cells. FRS2 expression was increased in nephroblastoma and served as a target of miR-562, moreover, FRS2 overexpression attenuated the inhibitory functions of miR-562 on the nephroblastoma cell malignant phenotypes mentioned above. Pre-clinically, lentivirus-mediated hsa_circ_0093741 silencing also impeded nephroblastoma tumor growth and metastasis *in vivo*.

Conclusion. Knockdown of hsa_circ_0093741 suppresses nephroblastoma cell growth, migration and invasion by regulating the miR-562/FRS2 axis, suggesting the potential involvement of hsa_circ_0093741 in nephroblastoma progression.

Corresponding Author: Jiang Yong, Department of Urology, Hunan Children's Hospital, The Paediatric Academy of University of South China Changsha, No.86 Ziyuan Road, Changsha City, Hunan Province, China. e-mail: yongjiang715@126.com

DOI: 10.14670/HH-18-539

Key words: Hsa_circ_0093741, miR-562, FRS2, Nephroblastoma, Migration

Introduction

Nephroblastoma, also known as Wilms' tumor, is an embryonic malignant solid kidney cancer that mostly occurs in children (Kanyamuhunga et al., 2015). It affects about 98% of children before the age of 10 years and occupies approximately 8% of pediatric cancers (Richards et al., 2017; Bazzaz et al., 2018). Although the overall survival rate of nephroblastoma patients is good (Apoznański et al., 2015), up to 25% of the patients are not able to be cured after diagnosis (Dome et al., 2013). It has been proposed that nephroblastoma may be the result of aberrant renal development (Hohenstein et al., 2015), therefore, in-depth explorations of the molecular and cellular mechanisms affecting the uncontrolled growth of nephroblastoma cells are indispensable.

Circular RNAs (circRNAs) are a kind of covalently noncoding RNAs formed by reverse-splicing (Hsiao et al., 2017). CircRNAs are abundant in various mammalian cells, and show high conservation and strong stability among organisms due to their covalent closed-loop structures (Rybak-Wolf et al., 2015), so they have better prospects for therapeutic application in human diseases (Han et al., 2018). Recently, increasing reports have proposed that circRNAs play an active role in modulating cell biological behaviors related to carcinogenesis, and moreover circRNAs have been observed to be differentially expressed and function as oncogenes or tumor suppressors in the progression of many types of cancers, including gastric cancer (Li et al., 2020), cervical cancer (Chen et al., 2019), breast cancer (Liu et al., 2019), even nephroblastoma (Zhou et al., 2021) and so on. Hsa_circ_0093741 is produced by back-splicing of the exon 6-9 of PCDH15 gene on chr10: 56089355-56138702 with a length of 548 nucleotides according to the annotation of circinteractome. In a previous study, Cao et al. proposed that hsa_circ_0093741 was significantly overexpressed

in nephroblastoma tissues by using the circRNAs microarray assay (Cao et al., 2021). However, the current research on hsa_circ_0093741 in nephroblastoma remains unclear.

Here, the functions of hsa_circ_0093741 on nephroblastoma tumorigenesis-related cell behaviors were investigated. It has been proposed that circRNAs can competitively bind to the microRNAs (miRNAs/miR) to regulate gene expression (Salmena et al., 2011; Hansen et al., 2013), thus, the miRNA/mRNA axis underlying hsa_circ_0093741 was studied to reveal the molecular mechanism.

Materials and methods

Clinical tissue specimens

Tumor tissues and matched non-cancer tissues were collected from 47 nephroblastoma patients who underwent surgery at Hunan Children's Hospital, the Paediatric Academy of University of South China Changsha, and then immediately snap-frozen in liquid nitrogen until use. Written informed consent has been provided by all patients, and this work was approved by the ethical committee of Hunan Children's Hospital, the Paediatric Academy of University of South China Changsha.

Cell culture

Human nephroblastoma cell lines (WiT49 and 17-94) and human renal tubular epithelial cell line (HK-2) were obtained from American Type Culture Collection (ATCC, Manassas, VA, USA) and cultured in high-glucose Dulbecco's modified eagle's medium (DMEM; Invitrogen, Carlsbad, CA, USA) harboring 10% fetal bovine serum (FBS, Invitrogen) and 1% penicillin/streptomycin (Solarbio, Shanghai, China) 37°C with 5% CO_2. WiT49 cell was derived from a primary lung metastasis of an aggressive nephroblastoma. 17-94 cell is an anaplastic nephroblastoma cell line that was established from the nephrectomy specimen of a large lobulated Wilms' tumor of a 4-year-old girl, expressing NCAM, SALL1, and CITED1, and containing a TP53 mutation.

Subcellular fractionation and quantitative real-time PCR (qRT-PCR)

The Cytoplasmic and Nuclear RNA Purification Kit (Norgen Biotek, Thorold, ON, Canada) was used to determine the RNAs from nuclear and cytoplasm fractions of WiT49 and 17-94 cells. Total RNAs were extracted from nephroblastoma tissues (Tissues were ground when frozen using Mortar and pestle) and cell lines (WiT49 and 17-94) using TRIzol reagent (Invitrogen). Approximately 3 μg of isolated RNAs were incubated with or without 4 U/μg of RNase R (Solarbio) for 3h at 37°C to determine the stability of circRNA. Total RNAs were then reverse transcribed into cDNA with PrimeScript RT Reagent Kit (Takara, Dalian, China). Thereafter, qRT-PCR analysis was conducted with SYBR Premix Ex Taq II (Takara). The relative fold changes were represented by CT value, and 18S rRNA, GAPDH or U6 were used as the internal reference. The specific primers are shown in Table 1.

Cell transfection

The transient transfection was implemented by using Lipofectamine 2000 provided by Invitrogen in target cancer cells. Two siRNAs targeting hsa_circ_0093741 (si-hsa_circ_0093741#1 and si-hsa_circ_0093741#2), pCD5-ciR/hsa_circ_0093741 overexpression plasmids (hsa_circ_0093741), pcDNA 3.1/FRS2 overexpression plasmids (FRS2) and the negative control (si-NC, circ-NC, or vector) were synthesized by Genema (Shanghai, China). The miR-562 mimic, inhibitor and their negative (NC or anti-NC) were procured from Ribobio (Guangzhou, China).

Cell counting Kit-8 (CCK-8) assay

After transfection, WiT49 and 17-94 cells were plated into a 96-well plate (2000 cells/well) and cultured for 0, 24, 48 or 72h. Then optical density values at 450 nm were read using a microplate reader after the additional incubation of 10 μL CCK-8 solution (Beyotime, Shanghai, China) in each well.

Colony formation assay

After 48h of transfection, WiT49 and 17-94 cells were seeded into a 6-well plate (500 cell/well) with complete medium and incubated for 14 days. The medium was replaced every three days after one week of culture. Finally, the colonies of cells were captured and counted after 0.1% crystal violet staining.

Table 1. Primers sequences used for qRT-PCR.

Name		Primers for qRT-PCR (5'-3')
hsa_circ_0093741	Forward	AGTGTTAAGGAAGAGGCTCAACT
	Reverse	TATGGTGGGGTCTGGTCCTC
PCDH15	Forward	GGATTGCAAACTAGCTAGGGGA
	Reverse	CAGAACTCTTCCGGTGCTGT
miR-562	Forward	GCCGAGAAAGTAGCTGTAC
	Reverse	CTCAACTGGTGTCGTGGAG
FRS2	Forward	CACAGAATGGGACACTGGCT
	Reverse	CCTACTTAGCTTGCGGGCTT
GAPDH	Forward	GACAGTCAGCCGCATCTTCT
	Reverse	GCGCCCAATACGACCAAATC
U6	Forward	CTCGCTTCGGCAGCACA
	Reverse	AACGCTTCACGAATTTGCGT
18S rRNA	Forward	CAGCCACCCGAGATTGAGCA
	Reverse	TAGTAGCGACGGGCGGTGTG

5-Ethynyl-2'-deoxyuridine (EdU) assay

WiT49 and 17-94 cells after assigned transfection were plated into a 96-well plate with complete medium containing 50 μM EdU labeling solution (Ribobio) and incubated for 2h. Then cells were fixed and permeabilized, and then stained with Apollo solution. Hoechst was used for cell nuclei staining. Finally, EdU-positive cells were measured using a fluorescence microscope (Bio-Rad, Hercules, CA, USA).

Transwell assay

Transfected WiT49 and 17-94 cells were suspended in 200 μL serum-free medium to adjust to 1×10^5 cells/mL and seeded into the upper chambers of a transwell insert (Corning, NY, USA) with a Matrigel-coated membrane. The lower chamber was filled with 600 μL medium harboring 20% FBS simultaneously. 24h later, invaded cells on the lower surface of membranes were captured and counted at 100× magnification using a microscope (Olympus, Tokyo, Japan).

Scratch assay

Transfected WiT49 and 17-94 cells were placed onto a 6-well plate for 24h, and then a scratch was generated in the middle of the wells by using a 200 μL pipette tip, followed by culturing in the serum-free medium. The width of wounds was imaged and measured at 0 and 24h in three-independent wound sites to assess cell migration.

Western blotting

Total proteins were exacted by using RIPA buffer (Beyotime) from nephroblastoma tissues (100 mg tissues/1 mL buffer) and cells (WiT49 and 17-94) (400 μL of 1x RIPA buffer/10 cm dish). Protein content was determined by a BCA method, separated by 10% SDS-PAGE and then electransferred onto a PVDF membrane (Bio-Rad). After blocking with 5% skimmed milk for 1 h, primary antibodies against PCNA (ab92552), MMP2 (ab92536), MMP9 (ab38898), and GAPDH (ab9485), obtained from Abcam (Cambridge, MA, USA), were used to incubate with the membranes at 4°C overnight, and then HRP-conjugated secondary antibody (ab6721, Abcam) was applied for secondary incubation at 37°C for 2h. Finally, the bands were detected by ECL detection reagent (Beyotime) and quantified using ImageJ.

Dual-luciferase reporter assay

The putative binding sequences and site-directed mutant sequences of miR-562 in hsa_circ_0093741 or FRS2 3'UTR were amplified and inserted into the pGL3-Basic vector (Promega, Madison, WI, USA) to generate wild-type (WT) or mutated (MUT) reporter vectors named as hsa_circ_0093741-wt/mut or FRS2-wt/mut. Then these constructed pGL3 vectors, pRL-TK Renilla plasmids and miR-562 mimic or mimic control were co-transfected into WiT49 and 17-94 cells, and firefly and Renilla luciferase activities were examined after 48h of transfection.

RNA immunoprecipitation (RIP) assay

WiT49 and 17-94 cells were homogenized in complete RNA lysis buffer and then incubated with magnetic beads conjugated with anti-Ago2 antibodies. Normal mouse IgG (Millipore) was used as the negative control. After interaction with Proteinase K, the immunoprecipitated RNAs were isolated and RNA levels were measured using qRT-PCR.

Tumor xenograft assay

All animal experiments were approved by Hunan Children's Hospital, the Paediatric Academy of University of South China Changsha Animal Care and Use Committee. Lentiviral plasmids carrying a

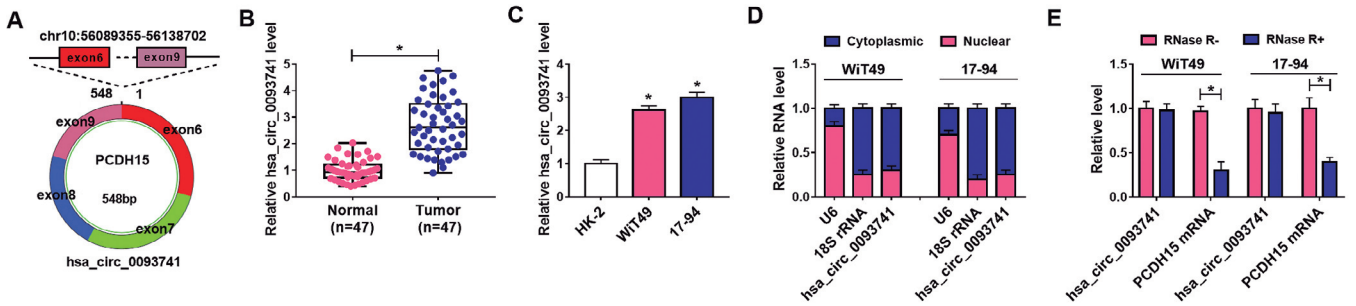

Fig. 1. Hsa_circ_0093741 is highly expressed in nephroblastoma tissues and cells. **A.** The genomic locus of the hsa_circ_0093741 and the back-spliced junction of hsa_circ_0093741 were indicated. **B, C.** qRT-PCR analysis of hsa_circ_0093741 expression level in nephroblastoma tissues and matched normal tissues, as well as in nephroblastoma tissues and cell lines (WiT49 and 17-94) and normal HK-2 cells. **D.** qRT-PCR analysis of hsa_circ_0093741 in the cytoplasm or the nucleus in WiT49 and 17-94 cells. **E.** qRT-PCR analysis of hsa_circ_0093741 and linear PCDH15 expression in WiT49 and 17-94 cells treated with or without RNase R. **P*<0.05.

scrambled control sequence (Lenti-sh-NC) or hsa_circ_0093741-specific short hairpin RNA (Lenti-sh-hsa_circ_0093741) were synthesized by Invitrogen. The stable transfected 17-94 cells were selected by puromycin at 0.5 μg/mL and then subcutaneously injected into randomized BALB/c nude mice (N=6/per group, six-weeks-old, Charles River Labs, Beijing, China). Tumor size was monitored every 5 days and the volume was calculated following the volume=(length×width2)/2. All mice were sacrificed at day 30, tumors were weighed and collected for either molecular analysis with qRT-PCR and western blotting or fixed in formalin for immunohistochemistry (IHC) analysis.

IHC staining

Paraffin sections of xenografts were deparaffinized and rehydrated, and then incubated with primary antibodies against ki-67 (ab15580), MMP2 (ab86607) and MMP9 (ab76003) at 4°C overnight, HRP-labeled streptavidin solution at 4°C for 30 min, followed by diaminoaniline (DAB) solution staining.

Statistical analysis

Quantitative data were presented as mean±standard deviation (SD). Statistical analyses were evaluated by using paired or unpaired Student's *t*-test, Mann-Whitney, or analysis of variance. The correlation between groups was determined by Pearson correlation. $P<0.05$ suggested statistical significance.

Results

Hsa_circ_0093741 is highly expressed in nephroblastoma tissues and cells

Hsa_circ_0093741 is produced by back-splicing of the exon 6-9 of PCDH15 gene on chr10: 56089355-56138702 with a length of 548 nt (Fig. 1A). The results of qRT-PCR showed that hsa_circ_0093741 expression was increased in nephroblastoma tissues compared with the adjacent normal tissues (Fig. 1B). Moreover, higher hsa_circ_0093741 expression was correlated with tumor size and advanced National Wilms Tumor Study (NWTS)-5 clinicopathologic stage ($P<0.05$, Table 2). Also, its expression was increased in nephroblastoma cell lines (WiT49 and 17-94) relative to the normal HK-2 cells (Fig. 1C). Then we detected the subcellular localization of hsa_circ_0093741 and found that hsa_circ_0093741 was mainly distributed in the cytoplasm of WiT49 and 17-94 cells (Fig. 1D). Moreover, it was observed that RNase R exoribonuclease was able to rapidly degrade linear PCDH15 rather than hsa_circ_0093741 in WiT49 and 17-94 cells, revealing the high stability of hsa_circ_0093741 (Fig. 1E). These data suggested that hsa_circ_0093741 is a stable circRNA and dysregulation of hsa_circ_0093741 might be associated with the progression of nephroblastoma.

Hsa_circ_0093741 silencing restrains nephroblastoma growth, invasion and migration in vitro

To determine the biological functions of hsa_circ_0093741 in nephroblastoma, two siRNAs targeting hsa_circ_0093741 were designed and transfected into WiT49 and 17-94 cells to conduct loss-of-function experiments. As expected, both the transfection of si-hsa_circ_0093741#1 and si-hsa_circ_0093741#2 significantly reduced hsa_circ_0093741 expression in WiT49 and 17-94 cells (Fig. 2A), and si-hsa_circ_0093741#1 was selected for subsequent analysis due to the highest knockdown efficiency. Functionally, hsa_circ_0093741 knockdown overly suppressed the growth of WiT49 and 17-94 cells, manifested by the decreased proliferation rates, colony forming abilities and DNA synthesis activities in cells (Fig. 2B-D). Furthermore, transwell and scratch assays revealed that hsa_circ_0093741 knockdown suppressed cell invasion and migration abilities in WiT49 and 17-94 cells (Fig. 2E-G). Then the related markers of cell behavior mentioned above were detected using western blotting, and we found that the levels of PCNA, MMP2, and MMP9 were markedly decreased after hsa_circ_0093741 down-regulation in WiT49 and 17-94 cells (Fig. 2H). Taken together, hsa_circ_0093741 might act as an oncogene to promote nephroblastoma progression.

Hsa_circ_0093741 functions as a sponge for miR-562

Given that hsa_circ_0093741 is mainly distributed in the cytoplasm in nephroblastoma cells, we speculated

Table 2. Correlation between hsa_circ_0093741 expression and clinicopathological characteristics of nephroblastoma patients.

Clinical feature		hsa_circ_0093741	
	n	High	Low
Gender			
Male	22	10	12
Female	25	14	11
Age (years)			
≥3	20	9	11
<3	27	15	12
Tumor size (cm)			
≥8	26	17	9
<8	21	7	14
Histological grade			
Favorable	19	9	10
Unfavorable	28	15	13
NWTS-5 Clinicopathologic stage			
I	18	5	13
II-V	29	19	10

NWTS-5: National Wilms Tumor Study-5.

that hsa_circ_0093741 might function as a miRNA sponge. According to the prediction of circinteractome database, miR-562 was predicted to possibly be a target of hsa_circ_0093741. The results of qRT-PCR analysis showed that miR-562 expression was decreased in nephroblastoma tissues and cells (Fig. 3A,C). More importantly, miR-562 expression was negatively correlated with hsa_circ_0093741 expression in tumor tissues (Fig. 3B). To confirm the binding between hsa_circ_0093741 and miR-562, we subsequently mutated the conserved target site of miR-562 on hsa_circ_0093741 (Fig. 3D) and cloned them into a luciferase reporter to conduct dual-luciferase reporter assay. The results showed that miR-562 mimics significantly decreased the luciferase activity of hsa_circ_0093741-wt luciferase reporter but not mutant one in WiT49 and 17-94 cells (Fig. 3E). Furthermore, RIP assay suggested that exogenous hsa_circ_0093741 and miR-562 were effectively pulled down by anti-Ago2 antibody relative to the control IgG in WiT49 and 17-94 cells (Fig. 3F). Thereafter, the transfection efficiency of hsa_circ_0093741 overexpression plasmids was validated by qRT-PCR (Fig. 3G). Then we found that miR-562 expression was decreased by hsa_circ_0093741 overexpression, but increased by hsa_circ_0093741 underexpression in WiT49 and 17-94 cells (Fig. 3H). Therefore, these results confirmed that hsa_circ_0093741 acted as a sponge for miR-562.

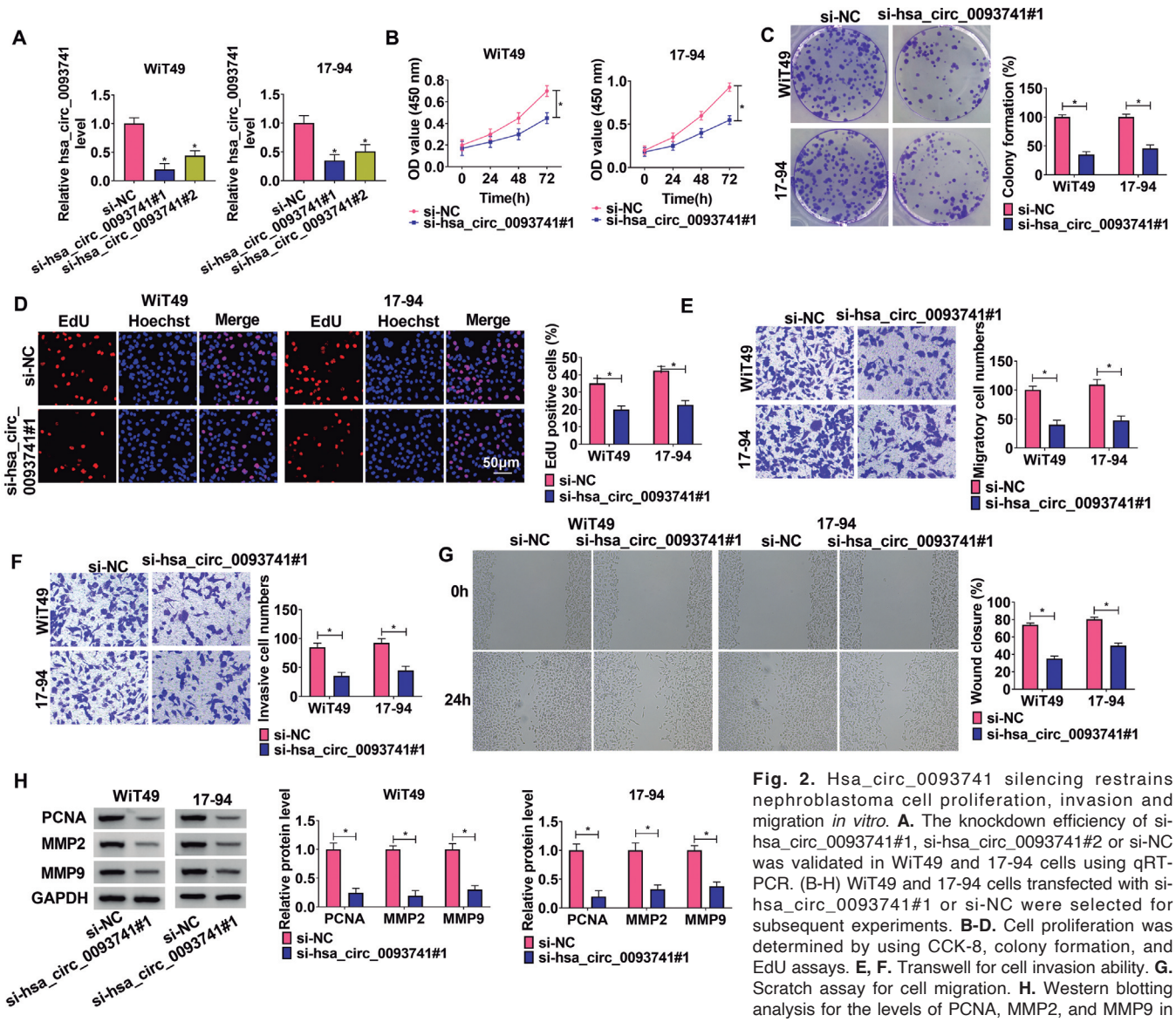

Fig. 2. Hsa_circ_0093741 silencing restrains nephroblastoma cell proliferation, invasion and migration *in vitro*. **A.** The knockdown efficiency of si-hsa_circ_0093741#1, si-hsa_circ_0093741#2 or si-NC was validated in WiT49 and 17-94 cells using qRT-PCR. (B-H) WiT49 and 17-94 cells transfected with si-hsa_circ_0093741#1 or si-NC were selected for subsequent experiments. **B-D.** Cell proliferation was determined by using CCK-8, colony formation, and EdU assays. **E, F.** Transwell for cell invasion ability. **G.** Scratch assay for cell migration. **H.** Western blotting analysis for the levels of PCNA, MMP2, and MMP9 in cells. **P*<0.05.

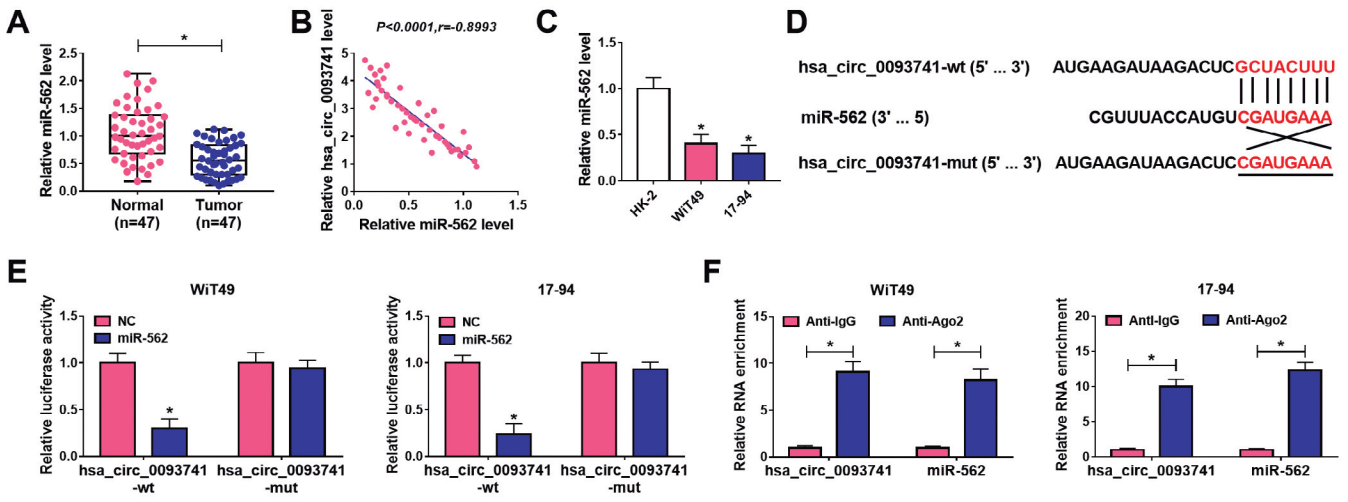

Fig. 3. Hsa_circ_0093741 functions as a sponge for miR-562. **A.** qRT-PCR analysis of miR-562 expression level in nephroblastoma tissues and matched normal tissues. **B.** miR-562 expression was negatively correlated with hsa_circ_0093741 expression in nephroblastoma tissues. **C.** qRT-PCR analysis of miR-562 expression level in nephroblastoma cell lines (WiT49 and 17-94) and normal HK-2 cells. **D.** The binding site between hsa_circ_0093741 and miR-562. **E, F.** The binding between hsa_circ_0093741 and miR-562 was verified using dual-luciferase reporter assay and RIP assays. **G.** The transfection efficiency of hsa_circ_0093741 and circ-NC was validated using qRT-PCR. **H.** The levels of miR-562 were detected using qRT-PCR in hsa_circ_0093741 decreased or increased WiT49 and 17-94 cells. **P*<0.05.

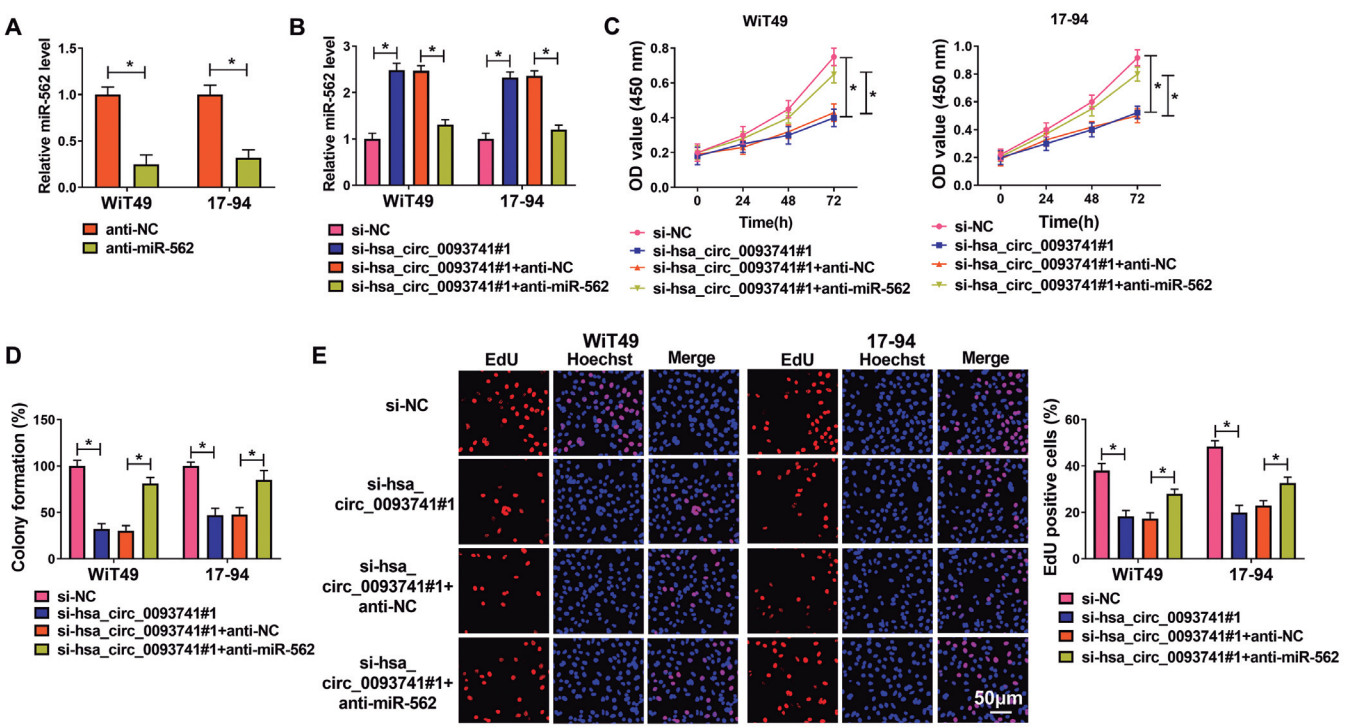

Fig. 4. Hsa_circ_0093741 silencing restrains nephroblastoma cell proliferation by regulating miR-562. **A.** The knockdown efficiency of anti-miR-562 or anti-NC. **B-E.** WiT49 and 17-94 cells were co-transfected with si-hsa_circ_0093741#1 and/or miR-562 inhibitor. **B.** qRT-PCR of miR-562 expression in cells after transfection. **C-E.** Cell proliferation was determined by using CCK-8, colony formation, and EdU assays. **P*<0.05.

Hsa_circ_0093741 silencing restrains nephroblastoma growth, invasion and migration by regulating miR-562

To determine whether miR-562 mediated the effects of hsa_circ_0093741 on nephroblastoma cells, the knockdown efficiency of miR-562 inhibitor was first validated by qRT-PCR (Fig. 4A). Then WiT49 and 17-94 cells were co-transfected with si-hsa_circ_0093741#1 and/or miR-562 inhibitor, and as expected, miR-562 inhibitor reversed the elevation of miR-562 levels caused by hsa_circ_0093741 silencing (Fig. 4B). Subsequently, a series of rescue experiments were performed. It was proved that miR-562 inhibitor abolished hsa_circ_0093741 silencing-evoked suppression of WiT49 and 17-94 cell proliferation (Fig. 4C-E), manifested by CCK-8, colony formation and EdU assays. Besides that, the reduction of the invasion and migration in WiT49 and 17-94 cells mediated by hsa_circ_0093741 silencing was also attenuated after miR-562 inhibition (Fig. 5A-D). Moreover, hsa_circ_0093741 silencing-induced decrease of PCNA, MMP2, and MMP9 levels in WiT49 and 17-94 cells was also rescued by the transfection of miR-562 inhibitor (Fig. 5E). Altogether, hsa_circ_0093741 was able to regulate nephroblastoma progression by targeting miR-562.

FRS2 is a target of miR-562, and hsa_circ_0093741 can regulate FRS2 through miR-562

The underlying targets of miR-562 were then searched. Targetscan database showed that FRS2 might be a target of miR-562. FRS2 was discovered to be increased in nephroblastoma tissues both at mRNA and protein levels (Fig. 6A,B). Moreover, FRS2 expression was positively correlated with hsa_circ_0093741 (Fig. 6C), but negatively correlated with miR-562 (Fig. 6D) in tumor samples. Similarly, FRS2 expression was also elevated in WiT49 and 17-94 cells (Fig. 6E). Therefore, we assumed that there might be a hsa_circ_0093741/miR-562/FRS2 axis in nephroblastoma. To verify this hypothesis, the putative binding sequences and site-directed mutant sequences of miR-562 in FRS2 3'UTR were cloned into a luciferase reporter (Fig. 6F).

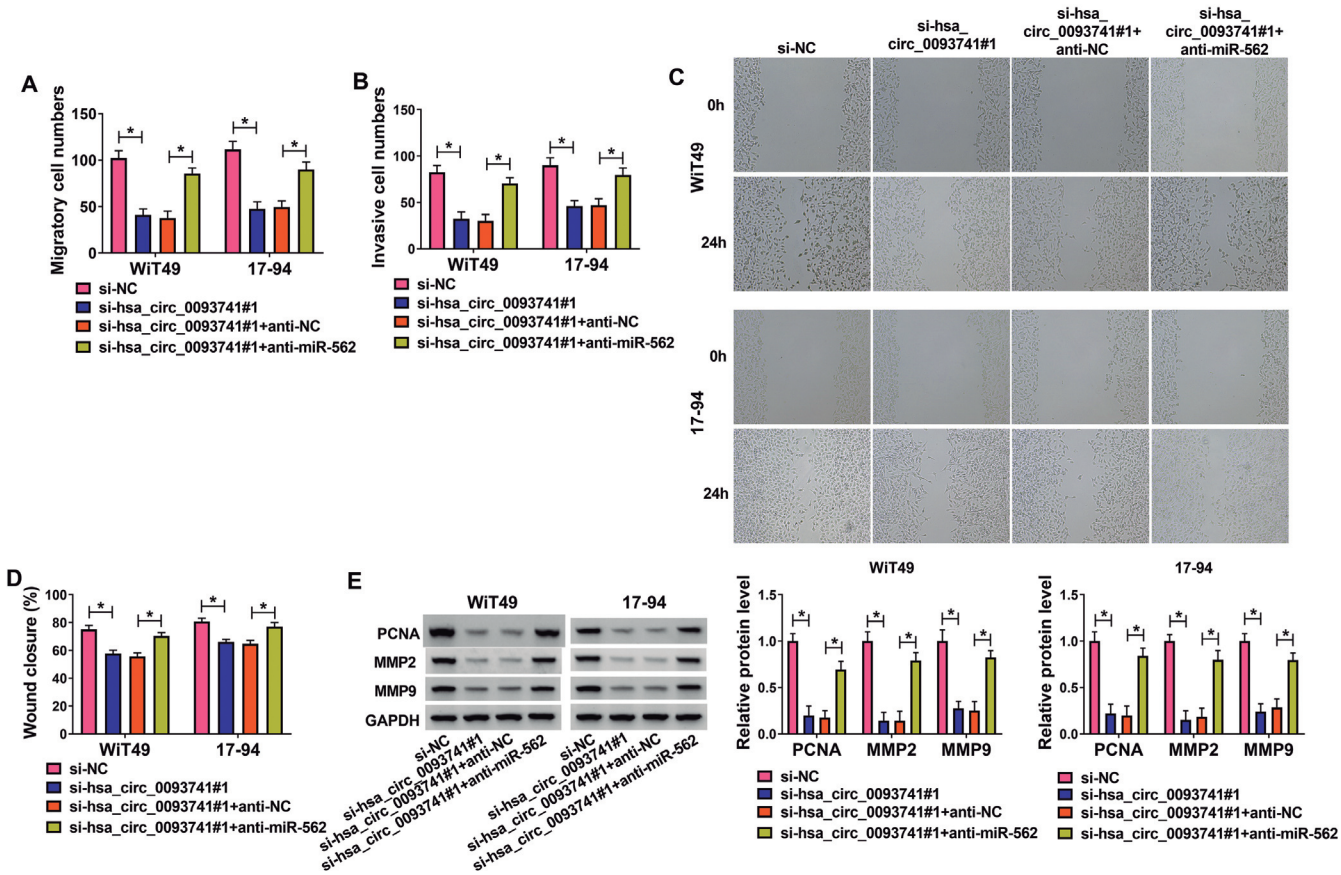

Fig. 5. Hsa_circ_0093741 silencing restrains nephroblastoma cell invasion and migration by regulating miR-562. **A-E.** WiT49 and 17-94 cells were co-transfected with si-hsa_circ_0093741#1 and/or miR-562 inhibitor. **A, B.** Transwell for cell invasion ability. **C, D.** Scratch assay for cell migration. **E.** Western blotting analysis for the levels of PCNA, MMP2, and MMP9 in cells. **P*<0.05.

Then the results of dual-luciferase reporter assay showed that the luciferase activity of FRS2-wt luciferase reporter was significantly reduced after miR-562 overexpression, while miR-562 mimic failed to affect the luciferase activity of the mutant one in WiT49 and 17-94 cells (Fig. 6G). The RIP assay also confirmed the interaction between miR-562 and FRS2 with the enrichment of miR-562 and FRS2 level in anti-Ago2 antibody group compared with the control IgG group in WiT49 and 17-94 cells (Fig. 6H). Thus, these data validated that miR-562 targeted FRS2. Besides that, we also observed that hsa_circ_0093741 knockdown led to a decrease of FRS2 expression level, which was rescued by the additional down-regulation of miR-562 in WiT49 and 17-94 cells (Fig. 6I), revealing the hsa_circ_0093741/miR-562/FRS2 feedback loop in nephroblastoma.

MiR-562 suppresses nephroblastoma growth, invasion and migration by regulating FRS2 expression

Subsequently, the biological functions of miR-562/FRS2 axis in nephroblastoma were explored. The transfection efficiencies of miR-562 mimic and FRS2 overexpression plasmids were first validated by using qRT-PCR and western blotting (Fig. 7A,B). Then it was observed that miR-562 mimic reduced FRS2 expression, while this effect was abolished by FRS2 vector transfection in WiT49 and 17-94 cells (Fig. 7C). Functionally, we proved that miR-562 mimic led to the suppression of WiT49 and 17-94 cell proliferation, which was reversed by FRS2 overexpression (Fig. 7D-F). Thereafter, the migration and invasion abilities of WiT49 and 17-94 cells were found to be impaired by

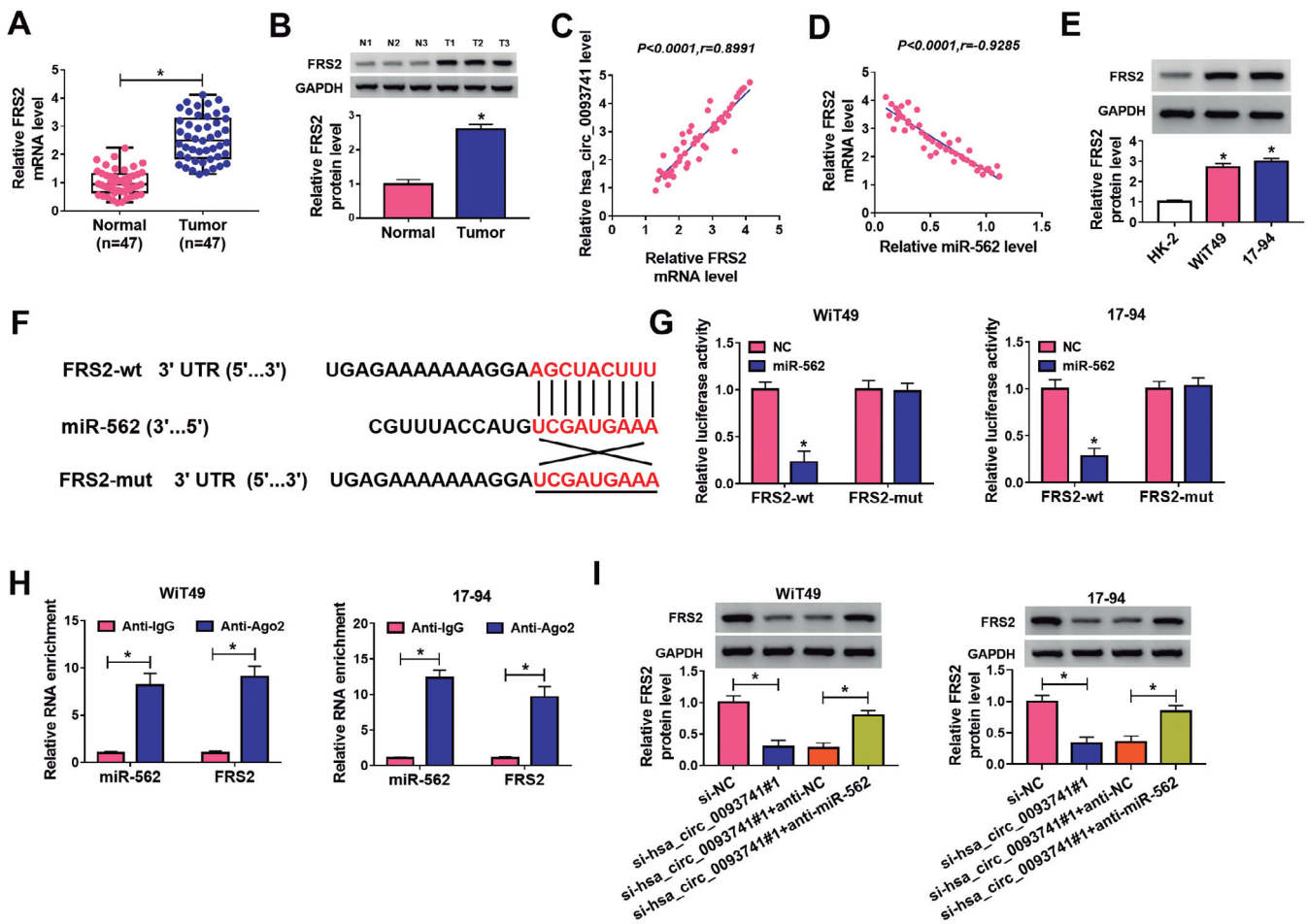

Fig. 6. FRS2 is a target of miR-562, and hsa_circ_0093741 can regulate FRS2 through miR-562. **A, B.** qRT-PCR and western blot analysis of the levels of FRS2 in nephroblastoma tissues and matched normal tissues. **C, D.** FRS2 expression was positively correlated with hsa_circ_0093741 expression and negatively correlated with miR-562 expression in nephroblastoma tissues. **E.** Western blotting analysis of FRS2 expression in nephroblastoma cell lines (WiT49 and 17-94) and normal HK-2 cells. **F.** The binding site between FRS2 and miR-562. **G, H.** The binding between hsa_circ_0093741 and miR-562 was verified using dual-luciferase reporter assay and RIP assays. **I.** The levels of FRS2 were detected using western blotting in WiT49 and 17-94 cells transfected with si-NC, si-hsa_circ_0093741#1, si-hsa_circ_0093741#1 + anti-NC, or si-hsa_circ_0093741#1 + anti-miR-562. **P*<0.05.

miR-562 mimic, and subsequently elevated in response to FRS2 vectors (Fig. 8A-D). Western blotting analysis showed that the levels of PCNA, MMP2 and MMP9 were decreased after miR-562 overexpression, which were rescued by the up-regulation of FRS2 (Fig. 8E). These results confirmed that miR-562 was able to regulate nephroblastoma tumorigenesis by FRS2.

Knockdown of hsa_circ_0093741 impedes nephroblastoma growth in vivo

To determine the effects of hsa_circ_0093741 on tumor growth *in vivo*, a tumor xenograft model in nude mice was established. The nephroblastoma markers WT1 and CD56 were detectable in the nephroblastoma xenografts, and a reduction of their activities was observed in tumors derived from Lenti-sh-hsa_circ_0093741 group. Then, it was demonstrated that the tumors derived from Lenti-sh-hsa_circ_0093741 group had smaller sizes and lower weights than tumors obtained from cells infected with Lenti-sh-NC (Fig. 9A,B). Besides, the results of qRT-PCR and western blotting showed that the levels of hsa_circ_0093741 and FRS2 were decreased, while the level of miR-562 was increased in tumor xenograft with decreased hsa_circ_0093741 (Fig. 9C,D). Western blotting analysis also showed the decrease of PCNA level in tumor xenograft with decreased hsa_circ_0093741 (Fig. 9D). Moreover, IHC staining showed the decreased expression of ki67, MMP2 and MMP9 in tumors derived from Lenti-sh-hsa_circ_0093741 group (Fig. 9E). Collectively, hsa_circ_0093741 acted as a sponge for miR-562 to up-regulate FRS2 expression, thus promoting nephroblastoma growth *in vivo*.

Discussion

Currently, with the advances in high-throughput technology, a large number of circRNAs are characterized and have been proven to play significant roles in multiple cellular processes (Zhang et al., 2018; Yu et al., 2019). Importantly, several circRNAs have been discovered to modulate nephroblastoma progression. For example, Zhou et al. proved that circCDYL stimulated TJP1 to impede nephroblastoma cell proliferation and mobility via sequestering miR-145-5p (Zhou et al., 2021). Circ0093740 was demonstrated to perform oncogenic effects in nephroblastoma by expediting nephroblastoma cell metastasis and growth through binding with the miR-136/145-DNMTA3 axis (Cao et al., 2021). However, large-scale identifications of circRNA expression in nephroblastoma tumorigenesis were not yet reported. In our study, we explored the role of hsa_circ_0093741 in nephroblastoma and found that hsa_circ_0093741 was highly expressed in nephroblastoma. Functionally, silencing of hsa_circ_0093741

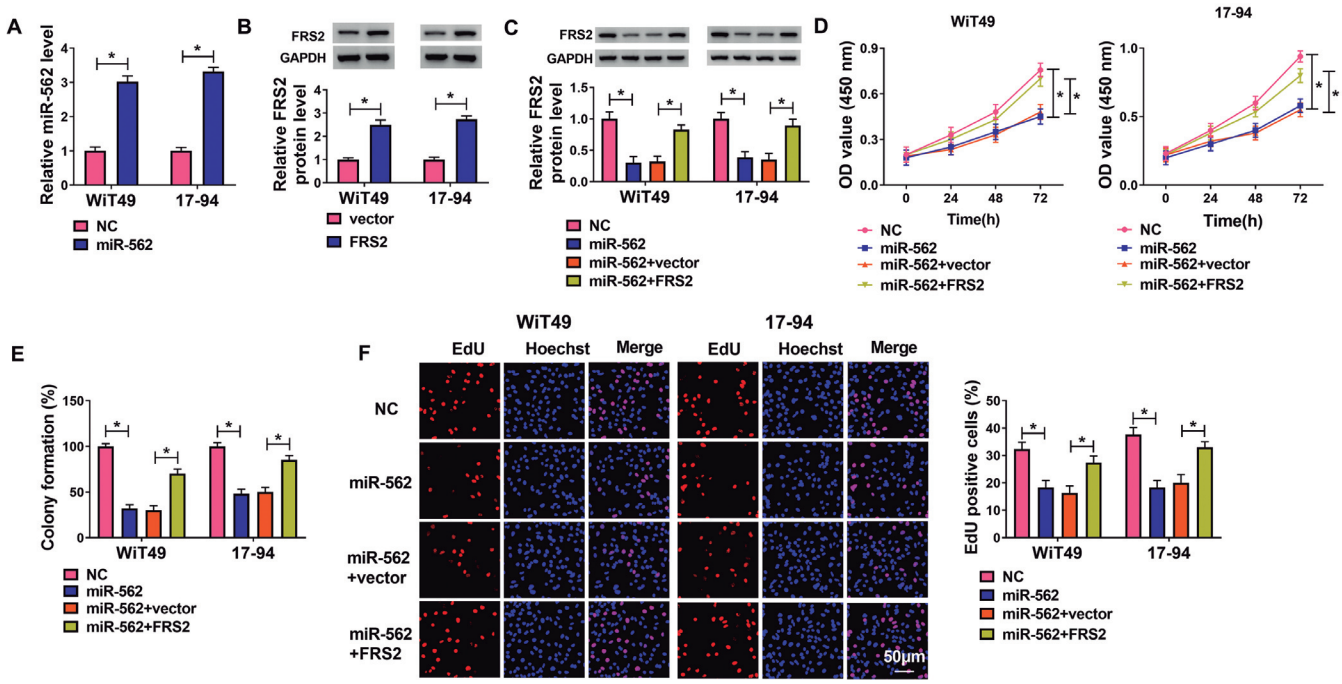

Fig. 7. MiR-562 suppresses nephroblastoma cell proliferation by targeting FRS2. **A, B.** The transfection efficiencies of miR-562 mimic and FRS2 overexpression plasmids were validated by using qRT-PCR and western blotting. **C-F.** WiT49 and 17-94 cells were transfected with NC, miR-562, miR-562 + vector, or miR-562 + FRS2. **C.** The expression levels of FRS2 were examined using western blotting. **D-F.** Cell proliferation was determined by using CCK-8, colony formation, and EdU assays. **P*<0.05.

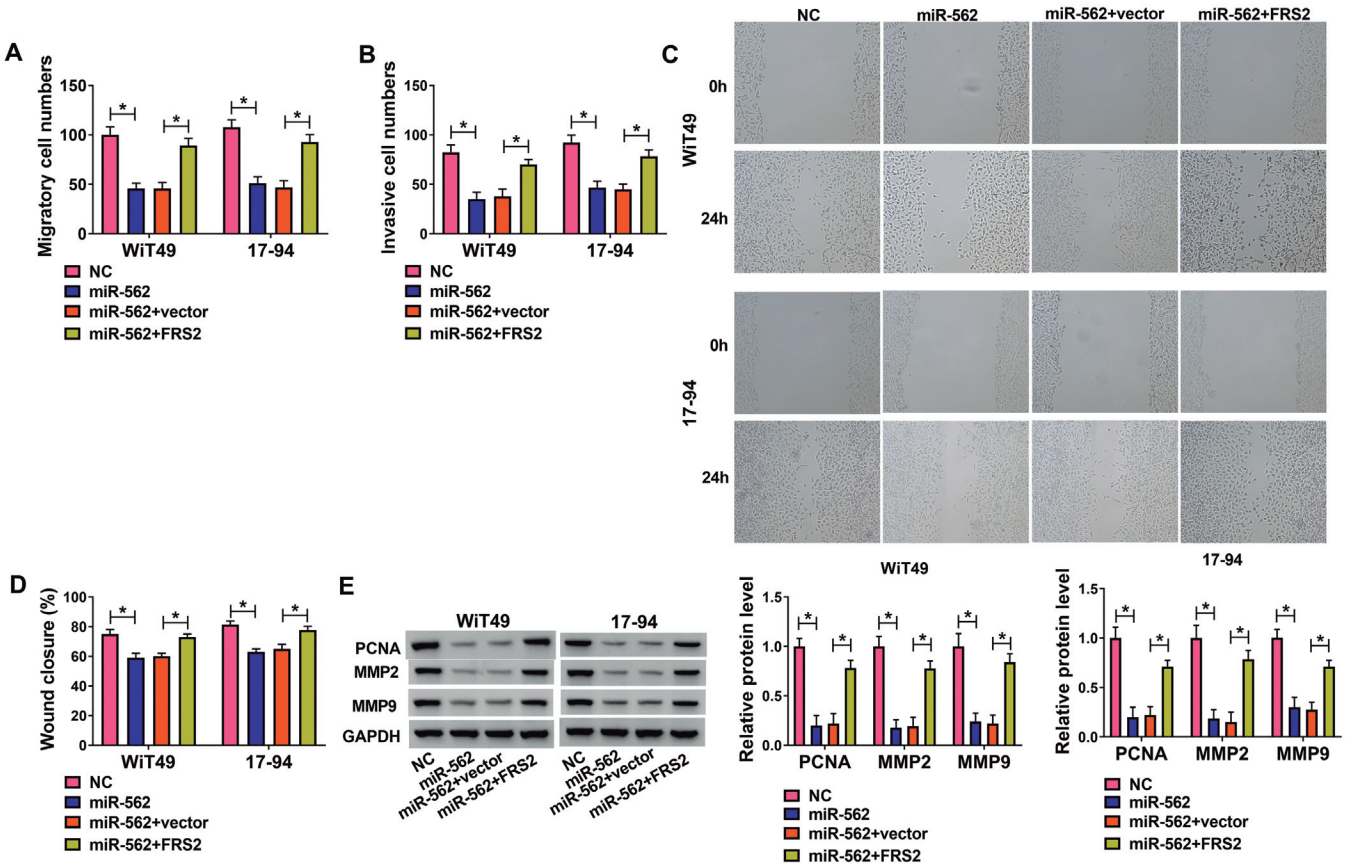

Fig. 8. MiR-562 suppresses nephroblastoma cell invasion and migration by FRS2. **A-E.** WiT49 and 17-94 cells were transfected with NC, miR-562, miR-562 + vector, or miR-562 + FRS2. **A, B.** Transwell for cell invasion ability. **C, D.** Scratch assay for cell migration. **E.** Western blotting analysis for the levels of PCNA, MMP2, and MMP9 in cells. **P*<0.05.

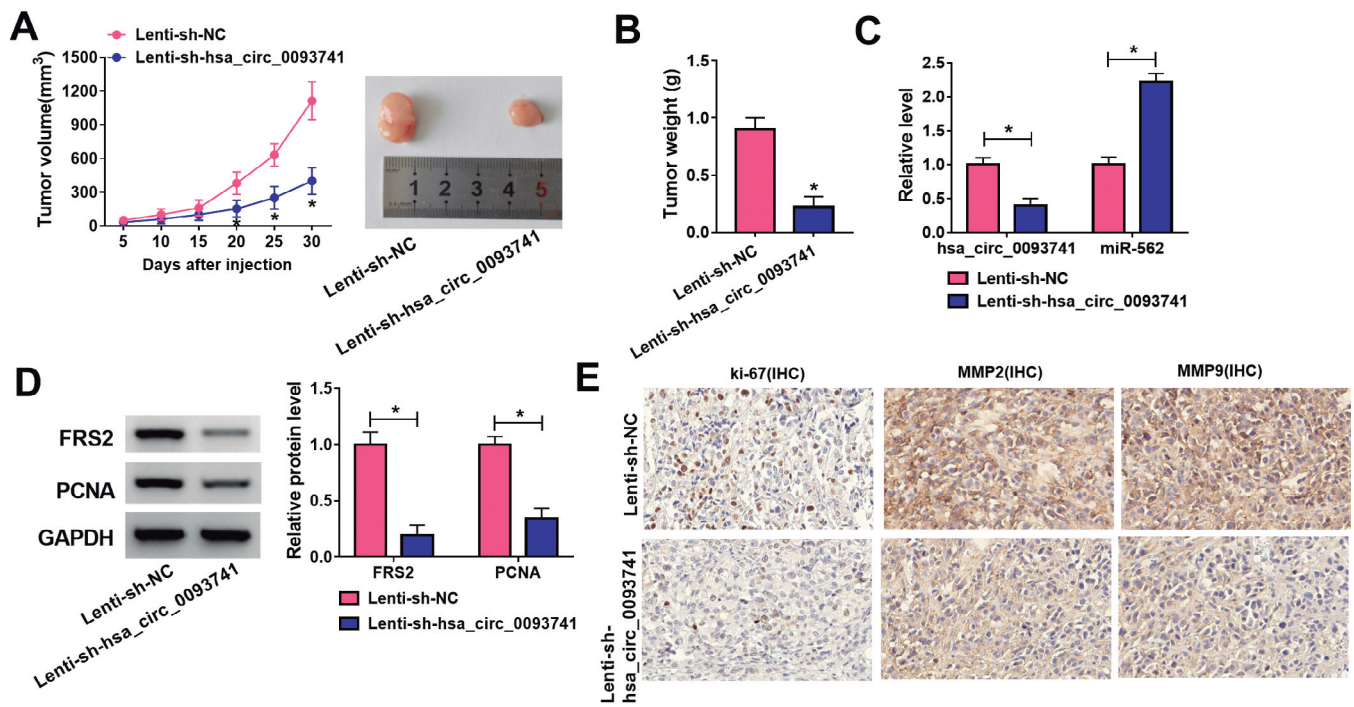

Fig. 9. Knockdown of hsa_circ_0093741 impedes nephroblastoma growth *in vivo*. **A.** Growth curves of xenograft tumors and the representative images of xenograft tumors of each group. **B.** Tumor weight of xenograft tumors of each group. **C.** The levels of hsa_circ_0093741 and miR-562 were measured by qRT-PCR in xenograft tumors of each group. **D.** Levels of FRS2 and PCNA were detected using western blotting in xenograft tumors of each group. **E.** IHE staining was applied to determine the protein levels of ki67, MMP2 and MMP9 in xenograft tumors of each group. **P*<0.05.

notably restrained nephroblastoma cell growth, invasion and migration. Moreover, consistent with the *in vitro* results, hsa_circ_0093741 silencing was demonstrated to hinder nephroblastoma growth and metastasis in nude mice. These results confirmed that hsa_circ_0093741 functioned as an oncogene in nephroblastoma and deletion of hsa_circ_0093741 might be an effective method to prevent nephroblastoma progression.

Our work showed that hsa_circ_0093741 is mainly distributed in the cytoplasm in nephroblastoma cells, thus, the underlying miRNAs interacting with hsa_circ_0093741 were investigated based on the competing endogenous RNA theory (Salmena et al., 2011; Hansen et al., 2013). We confirmed that miR-562 was a target of hsa_circ_0093741. MiR-562 is a functional miRNA. Nie et al. suggested that miR-562 had anti-proliferation properties in glioblastoma by repressing c-MET (Nie et al., 2019). However, Chen's team revealed that miR-562 was overexpressed and might positively regulate NSCLC progression via LINC01260/miR-562/CYLD/NF-κB pathway (Chen et al., 2020). All the findings suggested the complex action of miR-562 in cancer progression. Moreover, Drake et al. discovered that miR-562 was decreased and might be involved in the tumorigenesis of nephroblastoma by regulating EYA1 (Drake et al., 2009). Thereafter, we further assayed the role of miR-562 in nephroblastoma. A decreased expression of miR-562 was also observed in nephroblastoma, re-expression of miR-562 inhibited nephroblastoma cell growth and mobility and, importantly, the anticancer effects mediated by hsa_circ_0093741 knockdown were attenuated by miR-562 silencing.

In this work, we also verified that miR-562 directly targeted FRS2, meanwhile, hsa_circ_0093741 was able to regulate FRS2 expression by acting as a sponge for miR-562, indicating the hsa_circ_0093741/miR-562/FRS2 axis in nephroblastoma cells. Previous studies have shown that FRS2 has regulatory effects on cell biological behaviors such as cell differentiation, cycle arrest, cell growth and migration, and might act as an oncogene to regulate cancer progression (Valencia et al., 2011; Ren et al., 2014; Luo et al., 2015; Zhong et al., 2016). In nephroblastoma, FRS2 was revealed to function as a target of miRNAs, including miR-200c-3p (Li et al., 2019), miR-429 (Wang et al., 2022), miR-140-5p, miR-92a-3p (Li and Luo, 2020) and miR-613 (Wang et al., 2017), to mediate the malignant progression of this cancer, further indicating the oncogenic role of FRS2 in nephroblastoma. In our study, we showed an elevation of FRS2 in nephroblastoma, rescue experiments suggested that FRS2 attenuated the anticancer action of miR-562 in nephroblastoma.

In conclusion, our results indicated that hsa_circ_0093741 promoted WiT49 and 17-94 nephroblastoma cell proliferation and metastasis by regulating the miR-562/FRS2 axis, suggesting the potential involvement of hsa_circ_0093741 in nephroblastoma progression. However, this work was conducted using *in vitro* cell lines, and considering the shortcomings, further research should be carried out using primary nephroblastoma cells or nephroblastoma xenograft derived from primary cells to verify these conclusions, which may provide a valuable therapeutic target for nephroblastoma molecular therapy.

Acknowledgements. None.

Disclosure of interest. The authors declare that they have no conflicts of interest.

Funding. This work was supported by Hunan Provincial Health and Health Commission 2022 annual scientific research project (202204050012).

References

Apoznański W., Sawicz-Birkowska K., Palczewski M. and Szydełko T. (2015). Extrarenal nephroblastoma. Cent. European J. Urol. 68, 153-156.

Bazzaz N., Nouraee N., Zare-Mirzaie A., Shahali M., Mowla S.J. and Vasei M. (2018). MiR-21 Expression in Wilms' tumor. Iran J. Pathol. 13, 422-428.

Cao J., Huang Z., Ou S., Wen F., Yang G., Miao Q., Zhang H., Wang Y., He X., Shan Y., Liu S. and Jiang L. (2021). circ0093740 promotes tumor growth and metastasis by sponging miR-136/145 and upregulating DNMT3A in Wilms tumor. Front. Oncol. 11, 647352.

Chen R.X., Liu H.L., Yang L.L., Kang F.H., Xin L.P., Huang L.R., Guo Q.F. and Wang Y.L. (2019). Circular RNA circRNA_0000285 promotes cervical cancer development by regulating FUS. Eur. Rev. Med. Pharmacol. Sci. 23, 8771-8778.

Chen Y., Lei Y., Lin J., Huang Y., Zhang J., Chen K., Sun S. and Lin X. (2020). The LINC01260 functions as a tumor suppressor via the miR-562/CYLD/NF-κB pathway in non-Small cell lung cancer. Onco Targets Ther. 13, 10707-10719.

Dome J.S., Fernandez C.V., Mullen E.A., Kalapurakal J.A., Geller J.I., Huff V., Gratias E.J., Dix D.B., Ehrlich P.F., Khanna G., Malogolowkin M.H., Anderson J.R., Naranjo A. and Perlman E.J. (2013). Children's oncology Group's 2013 blueprint for research: renal tumors. Pediatr. Blood Cancer. 60, 994-1000.

Drake K.M., Ruteshouser E.C., Natrajan R., Harbor P., Wegert J., Gessler M., Pritchard-Jones K., Grundy P., Dome J., Huff V., Jones C. and Aldred M.A. (2009). Loss of heterozygosity at 2q37 in sporadic Wilms' tumor: putative role for miR-562. Clin. Cancer Res. 15, 5985-5992.

Han B., Chao J. and Yao H. (2018). Circular RNA and its mechanisms in disease: From the bench to the clinic. Pharmacol. Ther. 187, 31-44.

Hansen T.B., Jensen T.I., Clausen B.H., Bramsen J.B., Finsen B., Damgaard C.K. and Kjems J. (2013). Natural RNA circles function as efficient microRNA sponges. Nature 495, 384-388.

Hohenstein P., Pritchard-Jones K. and Charlton J. (2015). The yin and yang of kidney development and Wilms' tumors. Genes Dev. 29, 467-482.

Hsiao K.Y., Sun H.S. and Tsai S.J. (2017). Circular RNA - New member of noncoding RNA with novel functions. Exp. Biol. Med. (Maywood) 242, 1136-1141.

Kanyamuhunga A., Tuyisenge L. and Stefan D.C. (2015). Treating

childhood cancer in Rwanda: the nephroblastoma example. Pan Afr. Med. J. 21, 326.

Li J.L. and Luo P. (2020). MiR-140-5p and miR-92a-3p suppress the cell proliferation, migration and invasion and promoted apoptosis in Wilms' tumor by targeting FRS2. Eur. Rev. Med. Pharmacol. Sci. 24, 97-108.

Li T., Zhao P., Li Z., Wang C.C., Wang Y.L. and Gu Q. (2019). miR-200c-3p suppresses the proliferative, migratory, and invasive capacities of nephroblastoma cells via targeting FRS2. Biopreserv. Biobank. 17, 444-451.

Li R., Jiang J., Shi H., Qian H., Zhang X. and Xu W. (2020). CircRNA: a rising star in gastric cancer. Cell Mol. Life Sci. 77, 1661-1680.

Liu Z., Zhou Y., Liang G., Ling Y., Tan W., Tan L., Andrews R., Zhong W., Zhang X., Song E. and Gong C. (2019). Circular RNA hsa_circ_001783 regulates breast cancer progression via sponging miR-200c-3p. Cell Death Dis. 10, 55.

Luo L.Y., Kim E., Cheung H.W., Weir B.A., Dunn G.P., Shen R.R. and Hahn W.C. (2015). The tyrosine kinase adaptor protein FRS2 Is oncogenic and amplified in High-Grade serous ovarian cancer. Mol. Cancer Res. 13, 502-509.

Nie X., Su Z., Yan R., Yan A., Qiu S. and Zhou Y. (2019). MicroRNA-562 negatively regulated c-MET/AKT pathway in the growth of glioblastoma cells. Onco. Targets Ther. 12, 41-49.

Ren J., Huang H.J., Gong Y., Yue S., Tang L.M. and Cheng S.Y. (2014). MicroRNA-206 suppresses gastric cancer cell growth and metastasis. Cell Biosci. 4, 26.

Richards M.K., Goldin A.B., Savinkina A., Doski J., Goldfarb M., Nuchtern J., Langer M., Beierle E.A., Vasudevan S., Gow K.W. and Raval M.V. (2017). The association between nephroblastoma-specific outcomes and high versus low volume treatment centers. J. Pediatr. Surg. 52, 104-108.

Rybak-Wolf A., Stottmeister C., Glažar P., Jens M., Pino N., Giusti S., Hanan M., Behm M., Bartok O., Ashwal-Fluss R., Herzog M., Schreyer L., Papavasileiou P., Ivanov A., Öhman M., Refojo D., Kadener S. and Rajewsky N. (2015). Circular RNAs in the mammalian brain are highly abundant, conserved, and dynamically expressed. Mol. Cell. 58, 870-885.

Salmena L., Poliseno L., Tay Y., Kats L. and Pandolfi P.P. (2011). A ceRNA hypothesis: the Rosetta Stone of a hidden RNA language? Cell 146, 353-358.

Valencia T., Joseph A., Kachroo N., Darby S., Meakin S. and Gnanapragasam V.J. (2011). Role and expression of FRS2 and FRS3 in prostate cancer. BMC Cancer 11, 484.

Wang H.F., Zhang Y.Y., Zhuang H.W. and Xu M. (2017). MicroRNA-613 attenuates the proliferation, migration and invasion of Wilms' tumor via targeting FRS2. Eur. Rev. Med. Pharmacol. Sci. 21, 3360-3369.

Wang Y., Liu J., Yao Q., Wang Y., Liu Z. and Zhang L. (2022). LncRNA SNHG6 promotes Wilms' tumor progression through regulating miR-429/FRS2 axis. Cancer Biother Radiopharm. (in press).

Yu T., Wang Y., Fan Y., Fang N., Wang T., Xu T. and Shu Y. (2019). CircRNAs in cancer metabolism: a review. J. Hematol. Oncol. 12, 90.

Zhang H.D., Jiang L.H., Sun D.W., Hou J.C. and Ji Z.L. (2018). CircRNA: a novel type of biomarker for cancer. Breast Cancer 25, 1-7.

Zhong X., Xie G., Zhang Z., Wang Z., Wang Y., Wang Y., Qiu Y., Li L., Bu H., Li J. and Zheng H. (2016). MiR-4653-3p and its target gene FRS2 are prognostic biomarkers for hormone receptor positive breast cancer patients receiving tamoxifen as adjuvant endocrine therapy. Oncotarget 7, 61166-61182.

Zhou R., Jia W., Gao X., Deng F., Fu K., Zhao T., Li Z., Fu W. and Liu G. (2021). CircCDYL Acts as a tumor suppressor in Wilms' tumor by targeting miR-145-5p. Front. Cell Dev. Biol. 9, 668947.

Accepted October 26, 2022